

# Influence of deficit irrigation and warming on plant water status during the late winter and spring in young olive trees

Maria Agustina Iglesias<sup>a</sup>, M. Cecilia Rousseaux<sup>a,b</sup>, L. Martín Agüero Alcaras<sup>c</sup>, Leila Hamze<sup>a</sup>, Peter S. Searles<sup>a,\*</sup>

<sup>a</sup> Centro Regional de Investigaciones Científicas y Transferencia Tecnológica de La Rioja (CRILAR-Provincia de La Rioja-UNLaR, SEGEMAR-UNCa-CONICET), Entre Ríos y Mendoza s/n, Anillaco (5301), La Rioja, Argentina

<sup>b</sup> Departamento de Ciencias Exactas, Físicas y Naturales (DACEFyN), Universidad Nacional de La Rioja, Av. Luis M. de la Fuente s/n, Ciudad Universitaria de la Ciencia y de la Técnica, La Rioja (5300), La Rioja, Argentina

<sup>c</sup> Agencia de Extensión Rural Aimogasta, Instituto Nacional de Tecnología Agropecuaria (INTA), Ruta Nacional 60, Aimogasta (5310), La Rioja, Argentina

## ARTICLE INFO

### Keywords:

Global warming  
Irrigation  
*Olea europaea*  
Stem water potential  
Stomatal conductance

## ABSTRACT

Changes in rainfall patterns and increases in ambient air temperature (i.e., warming) are expected with climate change. Yet, little information is available on how plant water status will respond to the combination of water deficit and increased air temperature in fruit tree species. The objective of this study was to evaluate the individual responses of deficit irrigation and warming and their combination on plant water status during the late winter and spring in young olive trees. Two temperature and two irrigation levels were applied in open top chambers during the late winter and spring of 2018 and 2019 to two- or three-year-old, potted trees (cv. Arbequina in 2018; Coratina in 2019). The temperature levels were a near-ambient control and a warming treatment that was 4 °C above the control, while the two irrigation levels were 100% and 50% of irrigation needs. Midday stem water potential ( $\Psi_s$ ), stomatal conductance, net leaf photosynthesis, transpiration, and leaf temperature were measured periodically, and the difference between leaf and air temperature ( $\Delta T$ ) was calculated. The  $\Psi_s$  generally decreased due to irrigation deficit and warming when applied individually. When both treatments were combined, an additive response was observed. In contrast, stomatal conductance and net photosynthesis were consistently decreased by deficit irrigation, but were less affected by warming. Irrigation deficit did not affect leaf temperature under our experimental conditions. As was expected, warming most often increased leaf temperature, but it also significantly decreased  $\Delta T$  early in the season when leaf transpiration appeared to be greater due to warming. The results indicate that modifications in water management with global warming will likely be required given the mostly negative individual or additive effects of irrigation deficit and air temperature on  $\Psi_s$  and other variables.

## 1. Introduction

Climate change is expected to increase temperature and change rainfall patterns in many semi-arid regions (IPCC, 2021). Such changes will likely affect irrigation management in olive orchards and may negatively influence yields (Ferreira et al., 2011). Furthermore, the expansion of olive production towards regions with different climates from those of the Mediterranean Basin represents a challenge that requires a greater understanding of crop physiological and agronomic responses to the environment (Torres et al., 2017).

Currently, predictions on how carbon and water economy in olive

orchards will be affected by multiple global change variables are based mostly on models used to simulate different climate scenarios in the Mediterranean Basin rather than experimental field studies (e.g., Tanasijevic et al., 2014; Lorite et al., 2018; Fraga et al., 2020; Mairech et al., 2021). Such models have often indicated that the potentially negative effects of higher temperatures and less rainfall on photosynthesis and yield may be ameliorated by a beneficial response to the rising global CO<sub>2</sub> concentration and by increasing irrigation amounts. Nevertheless, a need to develop more sophisticated temperature sub-models has been identified (Mairech et al., 2021). Thus far, physiological leaf and whole plant responses to prolonged temperature increases have

\* Corresponding author.

E-mail addresses: [psearles@conicet.gov.ar](mailto:psearles@conicet.gov.ar), [psearles2@gmail.com](mailto:psearles2@gmail.com) (P.S. Searles).

<https://doi.org/10.1016/j.agwat.2022.108030>

Received 27 August 2022; Received in revised form 3 November 2022; Accepted 4 November 2022

Available online 18 November 2022

0378-3774/© 2022 The Authors. Published by Elsevier B.V. This is an open access article under the CC BY-NC-ND license (<http://creativecommons.org/licenses/by-nc-nd/4.0/>).

received little attention in olive trees. The available experimental evidence under well-watered conditions suggests some potential for maintaining leaf photosynthesis through thermal acclimation (i.e., physiological and biochemical adjustments), but less fruit and oil yield due to a change in carbon partitioning towards more vegetative growth (Miserere et al., 2019a, 2021). Additionally, water is a scarce resource in most olive growing regions, and likely will not always be available in greater amounts for irrigation due to other water demands.

Due to such concerns about water availability, deficit irrigation has often been evaluated in olive trees (see reviews by Fernández, 2014; Brito et al., 2019). Deficit irrigation consists of applying less than 100% of crop evapotranspiration (ETc) during certain phenological stages or throughout the growing season, and often allows for reducing irrigation without important decreases in yields (e.g., Iniesta et al., 2009; Correa-Tedesco et al., 2010; Agüero Alcaras et al., 2021). For deficit irrigation to be implemented, crop water status should be carefully measured to monitor the level of water stress. Direct methods for determining plant water status may include manual measurements of midday stem water potential ( $\Psi_s$ ) and stomatal conductance, or continuous, automatic measurements of sap flow and trunk diameter fluctuations (Fernández et al., 2011; Moriana et al., 2012; Agüero Alcaras et al., 2016; Ahumada-Orellana et al., 2019). Additionally, more indirect indicators of water status involving leaf temperature are often related to plant water status (Berni et al., 2009; Ben-Gal et al., 2009; García-Tejero et al., 2017).

At the end of the winter and early spring, large increases in evapotranspiration occur, which requires either the start of irrigation or an increase in irrigation amount and frequency. In the main olive growing regions of Argentina, most annual rainfall (100–400 mm) occurs in the summer months and irrigation throughout the entire year is a common management practice (Rousseaux et al., 2008; Pierantozzi et al., 2014). Additionally, average winter and spring temperatures in these growing regions are most often higher than those of the Mediterranean Basin (Searles et al., 2011; Torres et al., 2017). Finally, although irrigation in the spring is important for avoiding reductions in flowering and fruit set (Hueso et al., 2021), studies in the warm growing regions of Argentina suggest that some level of deficit irrigation can be appropriate in the spring in order to reduce excessive vegetative growth and pruning costs without incurring yield reductions (Trentacoste et al., 2019; Pierantozzi et al., 2020).

Compared to water deficit, less information is available about the plant water status responses of olive trees to air temperature under field conditions. Some studies have provided estimations by taking measurements over the course of the season as temperature changes or comparing locations with different temperature regimes. When the sap flow was measured at different times of the season, it was found to increase strongly above an average daily air temperature of 13 °C (Rousseaux et al., 2009). In addition,  $\Psi_s$  showed a negative linear relationship with daily maximum temperature across several locations in southern Spain (Corell et al., 2016).

To date, whole plant warming experiments in olive trees have only been conducted at a limited number of locations in the Mediterranean Basin (Vuletin Selak et al., 2013, 2014; Benlloch-González et al., 2018, 2019) and in Argentina (Miserere et al., 2019a; b, 2021, 2022). When warming the air by several degrees, either earlier or reduced flowering intensity has been found depending on the location as well as reduced fruit size, oil concentration (%), and oil yield per tree. At the leaf level, photosynthesis was not affected by warming (4 °C) during the oil accumulation phase, although increases in transpiration led to a decreased water use efficiency in warmed trees (Miserere et al., 2021). Sap flow of whole olive trees was greater after several months of warming than in control olive trees, and there was some evidence of thermal acclimation over the course of the season in that sap flow was greater in warmed trees when measured at the same temperature as control trees towards the end of the season (Miserere et al., 2019a). Unfortunately,  $\Psi_s$  was not measured in any of these previous studies.

Given the complexities of climatic change, there is a need for the simultaneous evaluation of multiple factors such as water deficit and warming under controlled experimental conditions (Suzuki et al., 2014; Jagadish et al., 2021). A short heat shock exposure (2 h at 40 °C) under controlled conditions strongly reduced leaf relative water content in both young well-irrigated and non-irrigated olive trees, while leaf photosynthesis was decreased more in the well-irrigated trees (Araújo et al., 2019). Similarly, although plant water status was not measured, a natural heat wave of several days in Italy with maximum daily temperature increasing from 31 °C to 41 °C decreased stomatal conductance and leaf photosynthesis in well-irrigated, potted olive trees, but not in trees receiving a water deficit (Haworth et al., 2018). Nevertheless, longer term warming studies with more moderate temperature increases that emulate the average temperature increase expected with global warming (2–4 °C) are still not available under different irrigation levels. Thus, the objective of this study was to determine the individual and combined responses of plant water status-related variables to deficit irrigation and moderate warming during the late winter and spring in young olive trees. Open top chambers (OTCs) were used for warming (3–4 °C) with two irrigation and two temperature levels.

## 2. Materials and methods

### 2.1. Plant material

The study was conducted during the late winter and spring of 2018 and 2019 (i.e., mid-August to late November) at the experimental field station of CRILAR-CONICET in La Rioja, Argentina (28° 48 'S latitude, 66° 56' W longitude; 1325 m above sea level). Two-year-old olive trees of cv. Arbequina were used in 2018 and three-year-old trees of cv. Coratina were used in 2019 based on tree availability. Leaf gas exchange and biomass of these two cultivars have been previously shown to respond similarly to warming under our experimental conditions (Miserere et al., 2021, 2022). The trees were provided by a commercial nursery (San Gabriel; La Rioja, Argentina), and they were transplanted at the field station into white, 30 l plastic pots during the spring of 2017. The trees were then grown outdoors in their own nursery until used in the experiment. The soil substrate was composed of sand, peat, and perlite (1: 1: 0.1, v/v) to obtain high water retention. The trees were watered daily in the nursery using drip irrigation to meet their water requirements based on previously reported sap flow and soil evaporation estimates (Rousseaux et al., 2009). Precipitation is uncommon during the winter and spring in this region. Fertilization was carried out manually once a month with macronutrients (15 N: 15 P: 15 K: 0.6 S) and once a week from flowering to harvest with micronutrients (0.02% B by weight; 0.01% Cu, 3% Fe, 1% Mn, 1%, Zn, 0.007% Mo) + nitrogen (2.8%) + magnesium (0.5%) (Aminoquelant minors, Brometan, Spain). The leaf area per tree was approximately 0.35 and 0.60 m<sup>2</sup> at the beginning and end of the experiment in 2018; respectively. In 2019, leaf area was 1.05 m<sup>2</sup> at the beginning and 1.25 m<sup>2</sup> at the end of the experiment. Flowering; and thus, fruit number was minimal the first year in the cv. Arbequina trees, but was greater the second season in cv. Coratina. Flowering occurred in early October, and pit hardening did not take place during the experimental periods.

### 2.2. Experimental design and treatments

The experimental design was a completely randomized design with two levels of both irrigation (equivalent to 100% and 50% of water consumed) and air temperature (a near-ambient control and a warming treatment of +4 °C). There were four replicates (n = 4) of each of the following four treatment combinations: 1) 100% irrigation, near-ambient temperature control (100 Tc); 2) 100% irrigation, warming treatment (100 T+); 3) 50% irrigation, near-ambient temperature control (50 Tc); and 4) 50% irrigation, warming treatment (50 T+). The entire experiment was conducted within 16 OTCs including four OTCs

for each combination of irrigation and temperature. Each OTC contained two potted olive trees that were placed within 30 cm-deep wells to reduce soil heating.

One of the two temperature levels was assigned to each OTC on approximately August 10 each year, which coincided with the start of new leaf growth in late winter. The near-ambient controls (Tc) had a target temperature of no more than 1 °C above the ambient, outdoor temperature, while the warming treatment (T+) had a target of 4 °C above Tc. The chambers were cube-shaped with dimensions of 2.0 m x 1.5 m x 1.5 m, and the side walls were covered by 150 µm thick polyethylene (Premium Thermal Agrotileño PLDT221510, AgroRedes, Argentina). The structure and plastic walls of the OTCs provided a similar microenvironment for both temperature levels including wind speed and light level (Miserere et al., 2019b).

The Tc OTCs were passively heated by the polyethylene sidewalls to some degree and were ventilated from outside the chamber by air that was released 20 cm above ground level under an air baffle in the center of each OTC. The top of the Tc OTCs was completely open, while the top of the T+ OTCs was partially covered with clear acetate (80 µm thick) to reduce the opening from 2.2 m<sup>2</sup> to 0.8 m<sup>2</sup> and increase heat retention. As described in Miserere et al. (2019b), two complementary heating systems were used for each T+ OTC including: 1) an external 6 m-long plastic sleeve containing black-painted stones that pulled heated air into each T+ OTC; and 2) an external electric heater with its own air ventilation system. The air temperature inside each OTC was recorded every 15 min with a data logger (Cavadevices, Buenos Aires, Argentina) by placing one temperature sensor (TC1047S, Microchip Inc. China) inside a protective solar radiation shield at tree canopy mid-height (1.0 m). The ambient, outdoor air temperature was also measured in the neighboring tree nursery located 30 m from the OTCs every 15 min at the same height. Lastly, data from an on-site weather station were used to determine absolute water vapor content in the air (g m<sup>-3</sup>), and subsequently to calculate the relative air humidity (RH; %) and vapor pressure deficit (VPD; kPa) for the given air temperature of each OTC. These values were verified by measuring RH every 15 min within one Tc OTC and one T+ OTC on some days using humidity sensors (Honeywell, model HIH 4000, USA).

After determining that the heating systems were functioning properly, the two irrigation levels were established on August 20, 10 days after the start of warming. Irrigation of the two trees within each OTC was applied using a pressurized drip irrigation system with a programmable electronic controller. There were two drip emitters per tree with a drip rate of 1.2 l h<sup>-1</sup> each for the OTCs receiving 100% of water consumed and one emitter (1.2 l h<sup>-1</sup>) per tree for the OTCs receiving deficit irrigation (50% of water consumed). Bubble-wrap insulation covered with aluminum foil (Aislamax, 10 mm thick, Buenos Aires, Argentina) was placed over both the soil surface and the drip emitters to reduce water loss and largely exclude any precipitation. To determine the daily amount of water consumed, two pots from each of the 100 Tc and 100 T+ temperature levels were weighed in the morning on two consecutive days twice a week using a precision balance (± 10 g; Moretti, Model MPF, Buenos Aires, Argentina). Irrigation was performed every 3 days to replace the water consumed. The 50 Tc and 50 T+ combinations received one-half of the irrigation of their respective 100% irrigation counterparts (100 Tc or 100 T+). In the second year, the irrigation applied to each pot was increased by 4% in October 2019 to account for the increased plant weight associated with spring growth.

### 2.3. Volumetric soil water content

Ten-cm-long capacitance sensors (ECHO-10, Decagon Devices, USA) were calibrated using two pots containing young olive trees before the start of the experiment. Two sensors per pot were inserted vertically at a depth of 5–15 cm, and the pots were then watered to excess. Without any further irrigation, soil samples of a known volume were then taken periodically and dried in a forced air oven at 105 °C to obtain volumetric

soil water content (%). These water content values were compared against sensor voltage output to obtain a linear calibration relationship ( $r^2 = 0.81$ ). Field capacity (45%) was determined 24 h after the watering, and permanent wilting point (5%) was approximated when the leaves of the potted trees became completely dry (Rapoport et al., 2012).

During the experiment, one soil moisture sensor was installed in each pot, and the sensors were connected to two 16-channel data loggers that recorded data hourly (Cavadevices, Buenos Aires, Argentina). The sensors were inserted vertically into the pots at a distance of 10 cm from the drip emitters at a depth between 5 and 15 cm. From the soil data, relative extractable water (REW, %) was calculated using the formula,  $REW = (R - R_{min}) / (R_{max} - R_{min})$ , where R is the current volumetric water content,  $R_{min}$  is the soil water content at the permanent wilting point, and  $R_{max}$  is the soil water content at field capacity (Gómez-del-Campo and Fernández, 2007).

### 2.4. Stem water potential

Midday stem water potential ( $\Psi_s$ ) was measured on five days during 2018 and seven days during 2019. The measurements were performed two days after irrigation on sunny days starting at solar noon (12:00 – 13:30 h solar time) using a Scholander-type pressure chamber (BioControl, Model 0–8 MPa, Buenos Aires, Argentina). One young stem located near the main trunk was selected per OTC ( $n = 16$ ) and covered with a plastic bag and aluminum foil at least 60 min before the measurement to obtain an equilibrium between the water potential of the stem and that of the trunk. Additionally, the water stress integral ( $S_{\Psi}$ , MPa\*day) during the treatment period was calculated. This integral provides an estimation of cumulative water stress in each treatment combination compared to the maximum  $\Psi_s$ , which was measured near the beginning of spring. The formula is:  $S_{\Psi} = |\sum (\Psi_s - c) * n|$ , where  $\Psi_s$  is the average of midday stem water potential between two consecutive measurement dates, c is the maximum  $\Psi_s$  measured during the season, and n is the number of days between measurements dates (Myers, 1988).

### 2.5. Leaf gas exchange

Stomatal conductance ( $g_s$ ) was measured on the same dates as  $\Psi_s$  using a porometer (Delta-T Devices, model AP4, Cambridge, UK). The measurements were performed during the morning (2–3 h before solar noon) on three, fully expanded leaves per OTC. The measured leaves were formed the previous growing season for the August, September, and early October measurements, while leaves from the current season that formed during the treatment period were used in all subsequent measurements. The  $g_s$  values on each date were measured in four Tc OTCs followed by all 8 T+ OTCs and then the last four Tc OTCs. Separate calibrations of the porometer were performed for the Tc and T+ OTCs. Briefly, the procedure involved fitting a curve of water vapor diffusion through six sets of holes of increasing diameter contained on a standardized calibration plate for the given relative humidity and air temperature conditions of the Tc or T+ OTCs. Net leaf photosynthesis at light saturation ( $A_{max}$ ) and transpiration (E) were also measured using a portable photosynthesis system (ADC BioScientific, model LCpro-SD, Hoddesdon, UK) on three dates during the treatment period in 2018 and 2019 along with one date each year after the treatment period. The measurements were performed during the morning (2–3 h before solar noon) on one fully expanded leaf per OTC. The air temperature in the leaf chamber was maintained similar to that of the OTC air temperature using a Peltier cooling system, and the measurement sequence was the same as that of the porometer. Each reading was taken on a known leaf area of 1.75 cm<sup>2</sup> after reaching stable  $A_{max}$  and E values about 1 min after placing the leaf in the chamber. The flow rate in the system was 200 µmol s<sup>-1</sup> and the photosynthetic photon flux density (PPFD) was greater than 1400 µmol m<sup>-2</sup> s<sup>-1</sup> for all measurements using natural ambient PPFD. From  $A_{max}$  and E, the instantaneous water use efficiency (WUE) was calculated as  $WUE = A_{max} / E$ . Although the portable

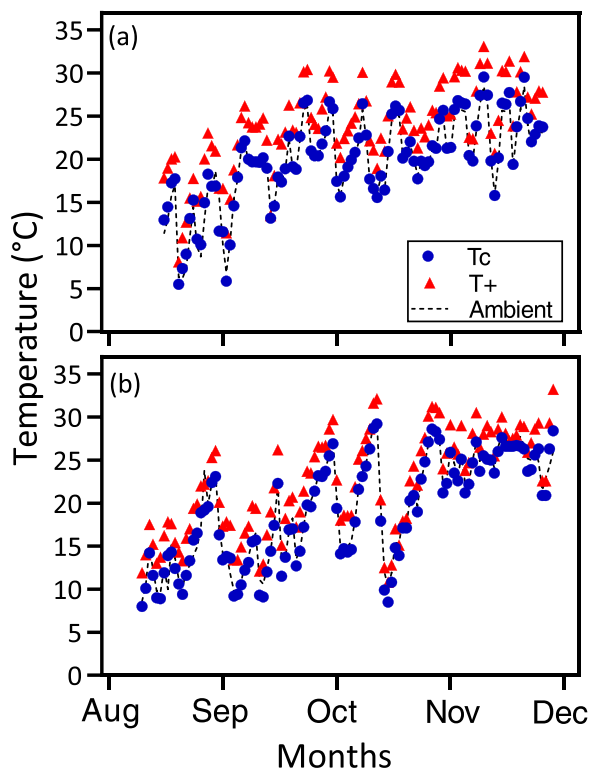


**Fig. 1.** Mean daily air temperature (°C) in the control (Tc) and warmed (T+) open top chambers (OTCs) and the ambient outdoor temperature during the treatments periods in (a) 2018 and (b) 2019. All temperatures were recorded at tree canopy mid-height (1.0 m). Symbols represent the average of eight independent OTCs.

photosynthesis system also calculates  $g_s$ , the porometer values are reported for this study because  $g_s$  with the porometer was measured on a greater number of measurement dates and using more leaves to obtain more robust averages with lower variability. Both instruments recorded similar average  $g_s$  values on most measurement dates.

## 2.6. Thermal imaging

Midday leaf temperature ( $T_{leaf}$ ) was determined on the same days and at approximately the same time (12:30 – 13:30 h solar time) as the  $\Psi_s$  measurements using images taken with an infrared thermal camera (Flir i40, Flir Systems, USA; 7–13  $\mu$ m spectral range, 120 × 120 pixels). One image per OTC was taken of well-illuminated foliage on the west-facing side of the tree canopy with a field of view of approximately 12.5 × 12.5 cm. The temperature of 20 leaves per image was analyzed with each pixel corresponding to an effective temperature reading with an emissivity ( $\epsilon$ ) of 0.96 (FLIR Tools software, Version 5.13.17214.2001). Based on  $T_{leaf}$  and simultaneous measurements of air temperature in each OTC, the difference between leaf and air temperature was calculated ( $\Delta T = T_{leaf} - T_{air}$ ). The  $T_{air}$  provided a reference for each image and was measured with a portable, digital temperature unit (Hygropalm 2, Rotronic Ag, NY, USA).

## 2.7. Statistical analyses

The potential effects of irrigation, temperature, and their interactions were determined for most variables ( $\Psi_s$ ,  $S_{\Psi}$ ,  $g_s$ ,  $A_{max}$ ,  $E$ ,  $WUE$ ,  $T_{leaf}$ ,  $\Delta T$ ) using standard factorial two-way analyses of variance (AgriColae package, R Core Team, 2020). When statistically significant effects were detected, differences among treatment means were assessed by Tukey tests ( $p < 0.05$ ). Daily values of relative extractable water were evaluated using linear mixed effects ANOVA models with irrigation,

**Table 1**

Averages of air temperature, relative air humidity, and vapor pressure deficit of control (Tc) and warmed (T+) open top chambers during the measurements (9:30–13:30 h solar time) of the plant water status-related variables. All temperatures were recorded at tree canopy mid-height (1.0 m). Values are means  $\pm$  SE ( $n = 8$  OTCs).

Year	Date	Air temperature (°C)		Relative air humidity (%)		Vapor pressure deficit (kPa)	
		Tc	T+	Tc	T+	Tc	T+
2018	Sept. 17	27.1 $\pm$ 0.5	31.1 $\pm$ 0.2	21.6 $\pm$ 0.5	17.3 $\pm$ 0.1	2.81 $\pm$ 0.10	3.73 $\pm$ 0.04
	Sept. 19 <sup>a</sup>	21.5 $\pm$ 0.3	26.1 $\pm$ 0.3	44.2 $\pm$ 0.8	33.4 $\pm$ 0.4	1.43 $\pm$ 0.05	2.25 $\pm$ 0.05
	Oct. 03	26.3 $\pm$ 0.2	30.9 $\pm$ 0.4	22.4 $\pm$ 0.3	17.4 $\pm$ 0.4	2.66 $\pm$ 0.04	3.68 $\pm$ 0.10
	Oct. 29	32.6 $\pm$ 0.6	37.1 $\pm$ 0.4	27.3 $\pm$ 0.8	21.5 $\pm$ 0.4	3.57 $\pm$ 0.15	4.96 $\pm$ 0.13
	Nov. 20	34.2 $\pm$ 0.5	38.1 $\pm$ 0.4	23.9 $\pm$ 0.6	19.5 $\pm$ 0.4	4.09 $\pm$ 0.14	5.37 $\pm$ 0.14
	Jan. 21 <sup>b</sup>	31.2		39.4		2.75	
	Aug. 28	30.9 $\pm$ 0.6	34.7 $\pm$ 0.4	29.1 $\pm$ 0.8	23.7 $\pm$ 0.5	3.16 $\pm$ 0.14	4.22 $\pm$ 0.11
	Sept. 13	22.7 $\pm$ 0.5	26.6 $\pm$ 0.4	28.8 $\pm$ 0.8	23.2 $\pm$ 0.6	1.97 $\pm$ 0.08	2.67 $\pm$ 0.09
	Sept. 30	34.7 $\pm$ 0.4	38.8 $\pm$ 0.2	19.2 $\pm$ 0.4	15.6 $\pm$ 0.2	4.48 $\pm$ 0.12	5.85 $\pm$ 0.07
	Oct. 25	31.5 $\pm$ 0.3	36.3 $\pm$ 0.4	24.6 $\pm$ 0.4	19.1 $\pm$ 0.4	3.57 $\pm$ 0.08	4.89 $\pm$ 0.12
2019	Nov. 15	33.8 $\pm$ 0.3	38.5 $\pm$ 0.2	27.9 $\pm$ 0.4	21.9 $\pm$ 0.3	3.79 $\pm$ 0.09	5.31 $\pm$ 0.08
	Nov. 29	35.5 $\pm$ 0.6	40.6 $\pm$ 0.4	19.7 $\pm$ 0.3	15.2 $\pm$ 0.3	4.64 $\pm$ 0.08	6.46 $\pm$ 0.16
	Dec. 06 <sup>b</sup>	28.5		20.4		3.10	

<sup>a</sup> Leaf photosynthesis and transpiration were not measured on Sept. 17 along with the other plant variables, but were measured 2 days later on Sept. 19 in 2018.

<sup>b</sup> Data on the last date shown for each year are for ambient, outdoor conditions after the treatment period.

temperature, and their interactions as fixed factors and plot as a random factor (nlme package, R Core Team, 2020). Potential relationships between  $\Psi_s$  as a function of  $T_{air}$  variables were assessed using linear regression (GraphPad Prism Software, LaJolla, CA, USA).

## 3. Results

### 3.1. Air temperature and irrigation

The average daily air temperature for the treatment period was 3.9 °C greater in the actively-heated OTCs (T+) than in the control OTCs (Tc) in 2018 with averages of 23.9 °C and 19.9 °C, respectively (Fig. 1a). Similarly, the air temperature was 3.2 °C greater in the T+ OTCs than in the Tc OTCs in 2019 (22.3 °C in T+, 19.1 °C in Tc) (Fig. 1b). In both years, the daily temperature within the Tc OTCs was within 1.0 °C of the ambient, outdoor temperature.

Depending on the day, the average air temperature in the Tc OTCs during the various plant measurements (09:30 – 13:30 solar time) ranged from 21.5° to 34.2 °C in 2018 and from 22.7° to 35.5 °C in 2019 (Table 1). The temperature in the T+ OTCs during the measurements was 4.3° and 4.4 °C higher on average than in the Tc OTCs in 2018 and 2019, respectively. Relative air humidity was generally low (15–44%) and was about 5% points lower in the T+ than the Tc OTCs. The VPD was 2.91 and 4.00 kPa in the Tc and T+ OTCs; respectively, during the measurements in 2018 with slightly higher values (3.60 kPa in Tc; 4.9 kPa in T+) in 2019. There was a 36% difference in VPD between the Tc and T+ OTCs, while the difference in air temperature was lower (15%).

The irrigation applied was 7% and 27% greater in 2018 and 2019; respectively, in 100 T+ than in 100 Tc based on the measurements of



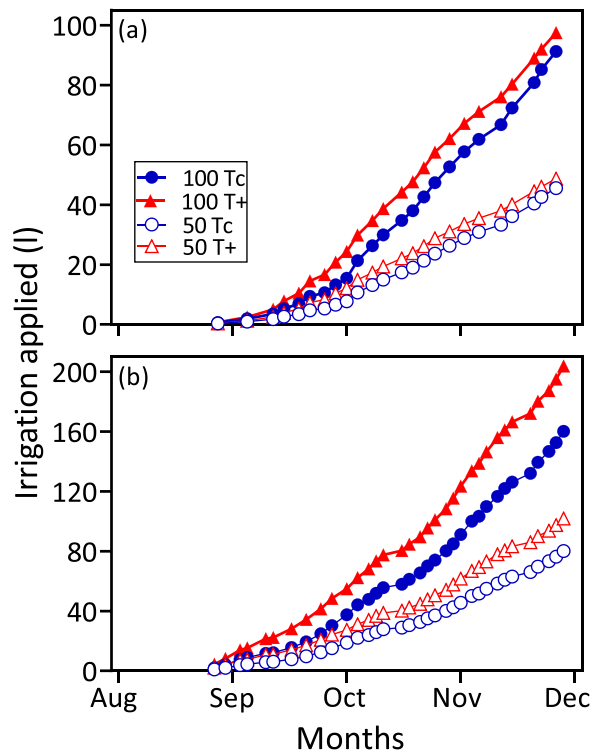


**Fig. 2.** Accumulated irrigation in the different irrigation (100%, 50%) and temperature (near-ambient control, Tc; warming treatment, T+) combinations in (a) two-year-old, cv. Arbequina trees in 2018 and (b) three-year-old, cv. Coratina trees in 2019. Each data point represents cumulative mean values for the two 100% irrigation combinations ( $n = 2$  OTCs per treatment combination). Irrigation of the 50% irrigation levels was calculated as one-half of the 100% irrigation levels.

**Table 2**

Average soil relative extractable water (REW; %) and the water stress integral ( $S_{\Psi}$ ) of the different irrigation (100%, 50%) and temperature (near-ambient control, Tc; warming treatment, T+) combinations during the entire treatment period in two-year-old, cv. Arbequina trees in 2018 and three-year-old, cv. Coratina trees in 2019. The values shown are means  $\pm$  SE ( $n = 4$  OTCs). The statistical probability level for irrigation and temperature are given as not significant (ns),  $p < 0.05$  (\*), and  $p < 0.01$  (\*\*). No interactions were found between factors.

Year	Treatment	REW (%)	Water stress integral ( $S_{\Psi}$ )
2018	100 Tc	74.5 $\pm$ 8.2	27.8 $\pm$ 4.3
	100 T+	80.0 $\pm$ 3.0	57.7 $\pm$ 5.3
	50 Tc	62.1 $\pm$ 4.1	44.6 $\pm$ 4.6
	50 T+	55.3 $\pm$ 7.1	78.4 $\pm$ 10.3
	p irri	*	*
	p temp	ns	**
2019	100 Tc	83.9 $\pm$ 12.5	72.7 $\pm$ 8.9
	100 T+	86.7 $\pm$ 1.7	133.4 $\pm$ 8.3
	50 Tc	68.0 $\pm$ 10.5	98.1 $\pm$ 7.3
	50 T+	67.5 $\pm$ 6.8	165.1 $\pm$ 5.9
	p irri	*	**
	p temp	ns	**

water consumed between consecutive days (Fig. 2). The 50 T+ and 50 Tc irrigation values were merely one-half of each corresponding 100% irrigation level.

### 3.2. Soil relative extractable water and stem water potential

As would be expected, the REW (%) for the entire treatment period during 2018 in cv. Arbequina was significantly lower in the 50%

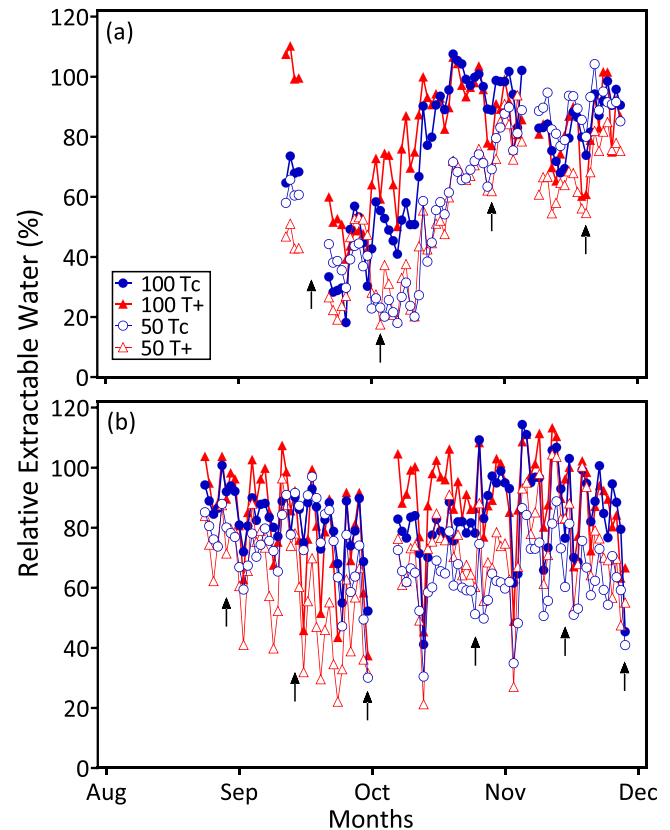


**Fig. 3.** Average daily values of soil relative extractable water (REW%) in the different irrigation (100%, 50%) and temperature (near-ambient control, Tc; warming treatment, T+) combinations in (a) two-year-old, cv. Arbequina trees in 2018 and (b) three-year-old, cv. Coratina trees in 2019. Each data point represents the daily mean ( $n = 4$  OTCs). Black arrows indicate the dates on which plant measurements were performed. Gaps between symbols represent unrecorded data.

irrigation treatment combinations (50 Tc, 50 T+) than in the 100% irrigation combinations (100 Tc, 100 T+) with averages of 58.7% and 77.3%, respectively ( $p < 0.05$ ; Table 2). Similar average differences in REW between the 50% and 100% irrigation treatment combinations were found during 2019 in cv. Coratina for the entire period. Although there was high variability in daily REW values, the lowest daily values ( $< 40\%$ ) during the two years were generally recorded in the 50% irrigation treatment combinations (Fig. 3). The REW values for the dates on which plant measurements were conducted were also significantly lower in the 50% irrigation treatment combinations in 2018 (51.1% for 50% irrigation, 69.2% for 100% irrigation;  $p < 0.05$ ) with a similar tendency in 2019 (61.1% for 50% irrigation, 75.3% for 100% irrigation;  $p < 0.08$ ).

The water stress integral ( $S_{\Psi}$ ) for the entire treatment period showed significant responses to both irrigation and temperature in 2018 and 2019 (Table 2). The control combination (100 Tc) had the lowest  $S_{\Psi}$  and the two T+ treatments (100 T+, 50 T+) had the highest  $S_{\Psi}$  in both years. As expected, no decrease in midday stem water potential ( $\Psi_s$ ) due to irrigation was apparent at the beginning of the treatment period, but a decrease in  $\Psi_s$  occurred on most measurement dates under the 50% irrigation level under both temperature conditions (Tc, T+) in 2018 and 2019 (Fig. 4). Both warming treatments (100 T+, 50 T+) had the most negative  $\Psi_s$  values during most of 2018 and 2019. After the treatments finished, no statistically significant differences in  $\Psi_s$  were observed when measured either two months after the treatments in 2018 or 8 days after in 2019. The recovery measurements were delayed in 2018 due to an unexpected torrential downpour and flooding event that saturated the soil of many pots.

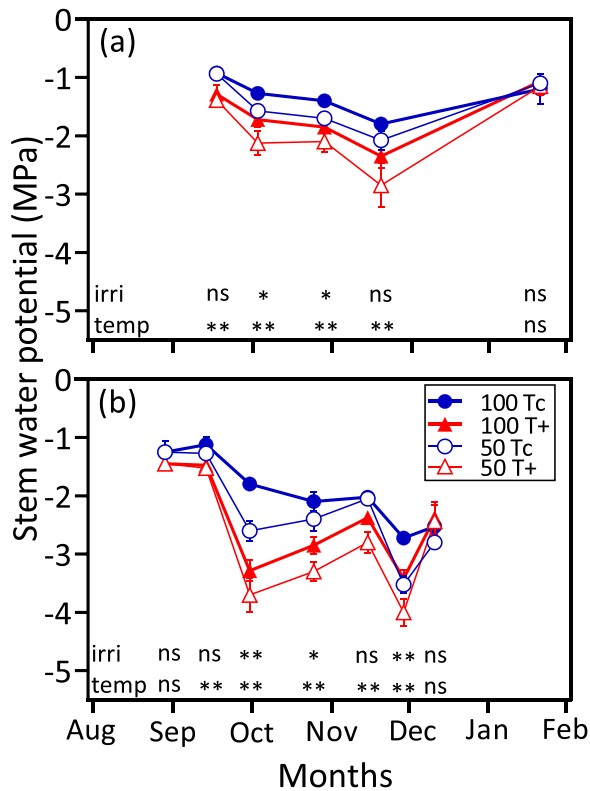


**Fig. 4.** Midday stem water potential ( $\Psi_s$ ) in the different irrigation (100%, 50%) and temperature (near-ambient control, Tc; warming treatment, T+) combinations in (a) two-year-old, cv. Arbequina trees in 2018 and (b) three-year-old, cv. Coratina trees in 2019. Each data point represents a mean  $\pm$  SE ( $n = 4$  OTCs). The statistical probability level for irrigation and temperature are given as not significant (ns),  $p < 0.05$  (\*), and  $p < 0.01$  (\*\*). No interactions were found between factors.

### 3.3. Stomatal conductance

The 50% irrigation level had consistently lower  $g_s$  values than the 100% irrigation level under both temperature regimes during the latter part of the treatment period in both years (Fig. 5). When the air temperature was low early in the season (Sept 13; Table 1) in 2019,  $g_s$  was greater under the warmed treatments (100 T+, 50 T+) than under Tc conditions (Fig. 5b). No consistent response to warming was observed when air temperature was higher. The 100 T+ treatment showed significantly higher  $g_s$  values compared to the other treatments on one date in 2018 (Fig. 5a), and T+ treatment combinations had lower  $g_s$  values than their corresponding Tc counterparts at each irrigation level on two dates in 2019 including the last date of the experimental period before recuperation was evaluated (Fig. 5b). In contrast to  $\Psi_s$ ,  $g_s$  was significantly lower at the 50% irrigation level than the 100% irrigation level when measured 8 days after full irrigation was restored in 2019, while  $g_s$  showed no remaining effect of the temperature treatments.

### 3.4. Net photosynthesis and transpiration

$A_{max}$  was also lower at the 50% irrigation level than the 100% level during the second half of the treatment period in both 2018 and 2019 (Fig. 6a, b). Decreases in  $E$  were not detected due to water deficit in 2018, but  $E$  was lower at the 50% irrigation level when measured on Nov 15 and Nov 29 in 2019 (Fig. 6c, d). Similar to  $g_s$ , both  $A_{max}$  and  $E$  remained lower at the 50% irrigation level in 2019 when measured 8 days after irrigation was restored (Fig. 6b, d). No significant effect of warming was observed on  $A_{max}$  in 2018 (Fig. 6a), but  $E$  was higher in late winter due to warming (Fig. 6c). The T+ treatments also showed

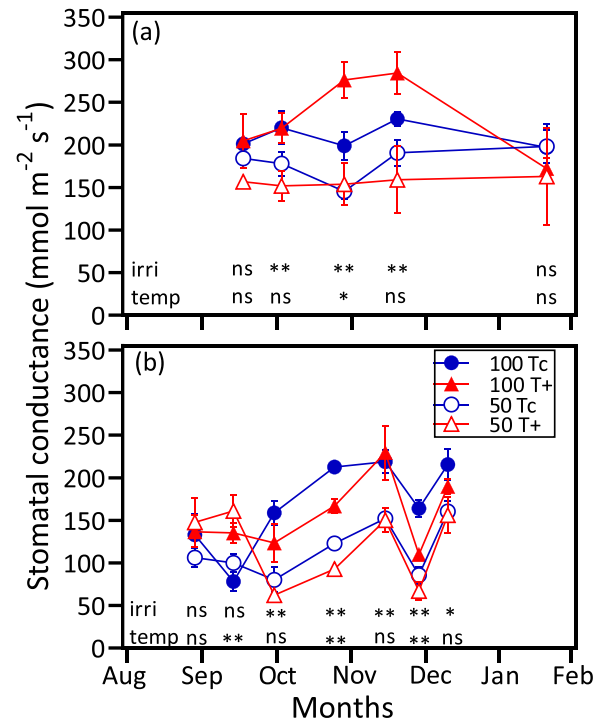


**Fig. 5.** Stomatal conductance ( $g_s$ ) in the different irrigation (100%, 50%) and temperature (near-ambient control, Tc; warming treatment, T+) combinations in (a) two-year-old, cv. Arbequina trees in 2018 and (b) three-year-old, cv. Coratina trees in 2019. Each data point represents a mean  $\pm$  SE ( $n = 4$  OTCs). The statistical probability level for irrigation and temperature are given as not significant (ns),  $p < 0.05$  (\*), and  $p < 0.01$  (\*\*). No interactions were found between factors.

higher  $E$  as well as  $A_{max}$  than the Tc treatments early in the season in 2019 when air temperatures were fairly low (Fig. 6b, d) as was observed for  $g_s$ . Later in the season (Nov 29) at higher temperatures, both  $A_{max}$  and  $E$  decreased significantly under T+ compared to Tc conditions, but they were mostly recovered under T+ when measured 8 days after the treatment period in 2019 ( $p \leq 0.10$ ).

The WUE ( $A_{max}/E$ ) was not affected by irrigation in either year during the treatment period (Fig. 6e, f). In contrast, the WUE was lower in T+ than in Tc for the first three measurement dates of 2018 (Fig. 6e), although no significant differences were found for WUE due to temperature in 2019 (Fig. 6f).

### 3.5. Midday leaf and air temperature

Irrigation level did not significantly affect either midday  $T_{leaf}$  or  $\Delta T$  during the treatment period in either year (Fig. 7). The  $T_{leaf}$  showed no differences between Tc and T+ at the beginning of the season, but higher  $T_{leaf}$  was observed in T+ for the remaining measurement dates during the treatment period in both years (Fig. 7a, b). In contrast,  $\Delta T$  was significantly lower in T+ than in Tc for both irrigation levels early in the season, while statistical differences were most often not detected later in the season (Fig. 7c, d). After the treatment period, midday  $T_{leaf}$  was similar in all treatments. When determining the relationship between midday  $T_{air}$  and  $T_{leaf}$  during the treatment period, the  $T_{leaf}$  was lower for a given  $T_{air}$  in the T+ treatments than in Tc in both years (Fig. 8). This difference was especially apparent at lower  $T_{air}$  in 2018 (Fig. 8a).

### 3.6. Relationships between stem water potential and air temperature

The  $\Psi_s$  was negatively related to midday air temperature with  $\Psi_s$  decreasing as air temperature increased (Fig. 9a, b). All of the treatment combinations were best fit to a single linear relationship in 2018 in cv.

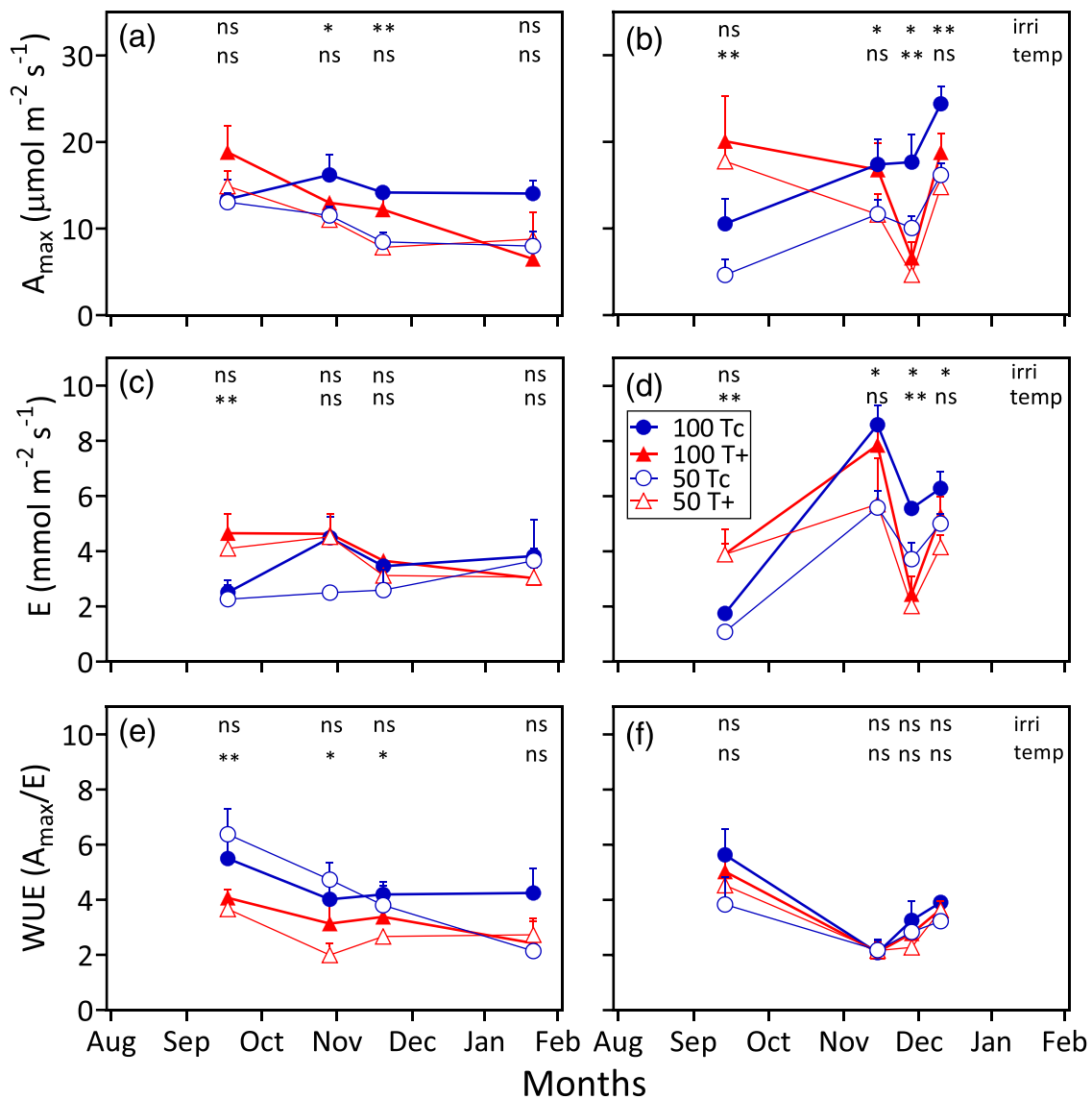


**Fig. 6.** Net leaf photosynthesis at light saturation ( $A_{\max}$ ; a, b), transpiration ( $E$ ; c, d), and water use efficiency ( $WUE$ ; e, f) in the different irrigation (100%, 50%) and temperature (near-ambient control, Tc; warming treatment, T+) combinations in (a, c, e) two-year-old, cv. Arbequina trees in 2018 and (b, d, f) three-year-old, cv. Coratina trees in 2019. Each data point represents a mean  $\pm$  SE ( $n = 4$  OTCs). The statistical probability level for irrigation and temperature are given as not significant (ns),  $p < 0.05$  (\*), and  $p < 0.01$  (\*\*). No interactions were found between factors.

Arbequina ( $R^2 = 0.48$ ; Fig. 9a). In 2019, the relationship between midday air temperature and 100 Tc ( $R^2 = 0.54$ ) had a similar y-intercept, but a lower slope than the other three treatment combinations (Fig. 9c). In addition,  $\Psi_s$  was negatively related to midday leaf temperature in both years (data not shown).

#### 4. Discussion

This is the first experimental study to assess the combination of deficit irrigation and warming in olive trees under natural temperature fluctuations over a prolonged period. As has been reported previously for this OTC design (Miserere et al., 2019b), active heating successfully increased daily  $T_{\text{air}}$  by 3–4 °C (Fig. 1), which was accompanied by a moderate increase in vapor pressure deficit of about 35%. In our continental Andean region, air temperatures are already higher than most olive growing regions (Searles et al., 2011; Hamze et al., 2022), and regional climate models predict that aridity will increase by mid-century (Zaninelli et al., 2019; Cabré and Nuñez, 2020). The cumulative irrigation applied was 7% and 27% greater during the experimental period

in 2018 and 2019; respectively, in the T+ OTCs than in the near-ambient control OTCs based on measurements of water consumed in the pots (Fig. 2). This confirms the postulated approach of Nissim et al. (2020) where young olive trees were irrigated one-third more at a high temperature site than at a moderate temperature site with a daily average temperatures difference of about 7 °C based on known evapotranspiration values at the two sites. Additionally, reducing the irrigation by 50% of the water consumed in the well-watered T+ and Tc pots was sufficient enough to obtain a moderate decrease in soil REW (Table 2; Fig. 3).

Midday  $\Psi_s$  is considered to be a good tool for monitoring plant water status and scheduling irrigation in olive and other fruit trees when the soil-plant-atmosphere continuum is properly considered (Moriana et al., 2012; García-Tejera et al., 2021; Shackel et al., 2021). In this study, deficit irrigation and warming combined to reduce  $\Psi_s$  (Fig. 4). The lower  $\Psi_s$  of the trees with deficit irrigation reflected the lower soil REW in the 50% treatments and warming further decreased  $\Psi_s$ . The decrease with the warming treatments is likely to be a function of the increased temperature accompanied by higher VPD in the T+ treatments. Experimental warming during the summer at our field location has previously

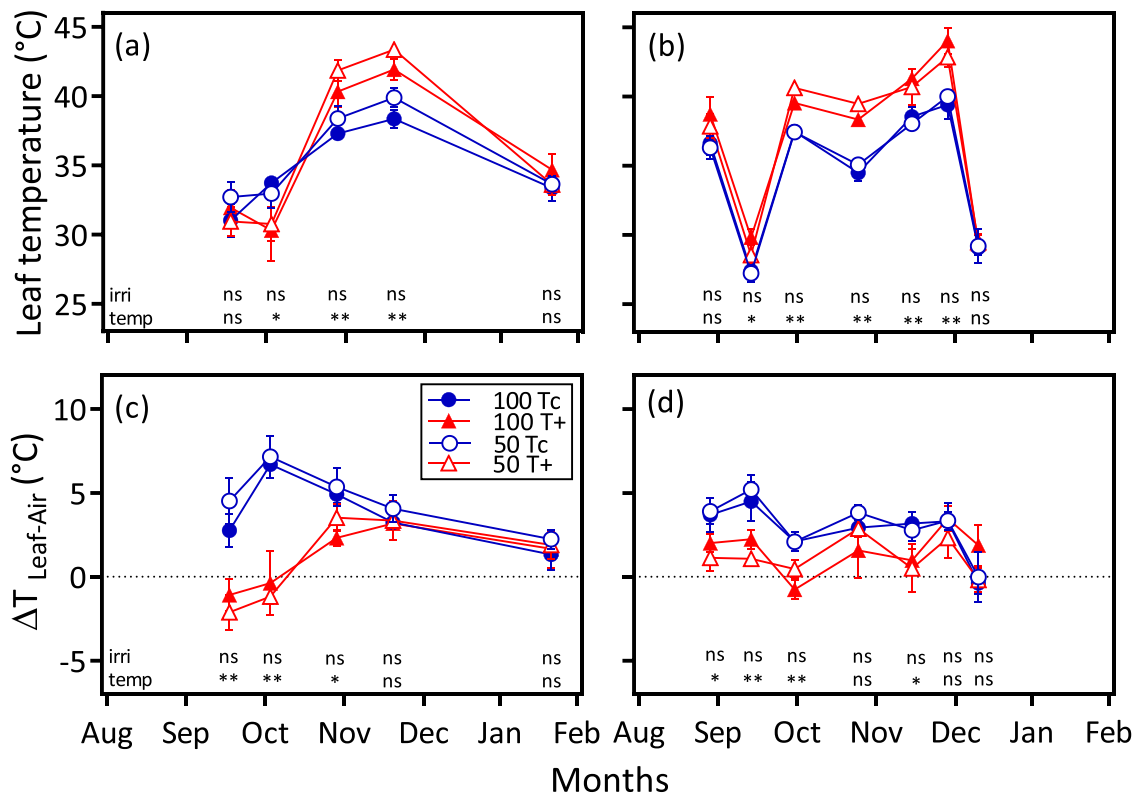


**Fig. 7.** Midday leaf temperature (a, b) and the difference between midday leaf and air temperature ( $\Delta T_{\text{leaf-air}}$ ; c, d) in the different irrigation (100%, 50%) and temperature (near-ambient control, Tc; warming treatment, T+) combinations in (a, c) two-year-old, cv. Arbequina trees in 2018 and (b, d) three-year-old, cv. Coratina trees in 2019. Each data point represents a mean  $\pm$  SE ( $n = 4$  OTCs). The statistical probability level for irrigation and temperature are given as not significant (ns),  $p < 0.05$  (\*), and  $p < 0.01$  (\*\*). No interactions were found between factors.

been shown to increase whole-tree sap flow and leaf transpiration on some measurement dates in young olive trees (Miserere et al., 2019a, 2021), which would lead to lower  $\Psi_s$ . Once the irrigation was restored and trees were returned to ambient temperature conditions, the  $\Psi_s$  recovered to control values as has been observed in several studies (Agüero Alcaras et al., 2016; Ahumada-Orellana et al., 2017; Martín-Palomo et al., 2021). When expressed as water stress integral ( $S_{\Psi}$ ), the greatest  $S_{\Psi}$  tended to be found in the 50 T+ treatment combination with about two-thirds of the greater  $S_{\Psi}$  being due to warming and only about one-third being due to deficit irrigation (Table 2). The large response of  $S_{\Psi}$  to warming shows the potential importance of warming (+4 °C) with climate change under both well-watered and water deficit conditions.

Stomatal control regulates both water and  $\text{CO}_2$  exchange in plants (Damour et al., 2010; Chaves et al., 2016), and reductions in  $g_s$  and  $A_{\text{max}}$  have often been shown in olive leaves under deficit irrigation (Fernández et al., 1997; Moriana et al., 2002; Ahumada-Orellana et al., 2019). As expected, the  $g_s$  and  $A_{\text{max}}$  were consistently reduced in the latter half of the treatment period in both years at the 50% irrigation level (Fig. 6). Interestingly, warming appeared to increase  $g_s$  as well as  $A_{\text{max}}$  and E near the beginning of spring on days with moderate ambient temperatures (Fig. 5b; 6). At this time, it is likely that the air temperature in Tc of slightly above 20 °C was sub-optimal for photosynthesis (Bongi et al., 1987; Diaz-Espejo et al., 2006). Later in the spring under higher temperatures, the responses to warming showed both an increase in  $g_s$  on one date in 2018 and some lower values in  $g_s$  and  $A_{\text{max}}$  in 2019. Using  $g_s$  values for an entire experimental period,  $g_s$  was not significantly related to air temperature in either year. In the summer at our field location,  $g_s$  also did not show a consistent response to warming (4 °C), and  $A_{\text{max}}$  was little affected (Miserere et al., 2021). In contrast,  $g_s$  decreased in cv. Coratina above 30 °C under controlled, laboratory conditions, but little decrease even up to 40 °C was found in some other cultivars (Bongi et al., 1987). A natural heat wave in Italy with maximum temperatures

about 10 °C above normal, drastically reduced  $g_s$  and net photosynthesis under well-watered conditions. However, they were not reduced when already low due to severe water stress (Haworth et al., 2018). These results emphasize that the magnitude and duration of temperature increases as well as cultivar characteristics are likely to strongly affect plant responses as suggested by Jagadish et al. (2021). Leaf age should also be carefully considered in further studies. Lastly, in contrast to  $\Psi_s$ , the recovery of the gas exchange variables in 2019 eight days after irrigation and ambient temperature were restored was not complete for the water deficit trees, which has also been reported by other authors (see review by Fernández et al., 2014; Ahumada-Orellana et al., 2022).

The use of thermal imagery as an indirect measurement of stress in olive trees is of considerable interest because of its potential use to monitor olive orchards by remote sensing (Sepulcre-Cantó et al., 2006; Berni et al., 2009). When deficit irrigation leads to severe reductions in  $g_s$  in olive leaves, stomatal closure has been shown to result in an increase of about 2 °C in the tree canopy temperature relative to the air temperature because leaf cooling is reduced (García-Tejero et al., 2017). In our study, no significant increases in  $T_{\text{leaf}} - T_{\text{air}}$  were found when moderate reductions in  $g_s$  occurred in the 50% irrigation treatments (Fig. 7c, d). The fairly small size of olive leaves and their lanceolate leaf shape have been suggested to strongly contribute to coupling with the surrounding air (Villalobos and López-Bernal, 2017). Thus, detecting a moderate level of water stress may prove difficult in olive trees compared to some deciduous fruit trees with larger leaves. In contrast, the warmed treatments showed a lower  $T_{\text{leaf}} - T_{\text{air}}$  than the near-ambient temperature level in late winter and early spring when  $g_s$  and E were sometimes greater in T+ (Fig. 5b; 6c, d), which could have contributed to leaf cooling in T+. Later in the spring, no clear differences between treatments in  $T_{\text{leaf}} - T_{\text{air}}$  were apparent in either year.

Understanding the relationships between environmental variables such as air temperature and plant water status is critical for crop water



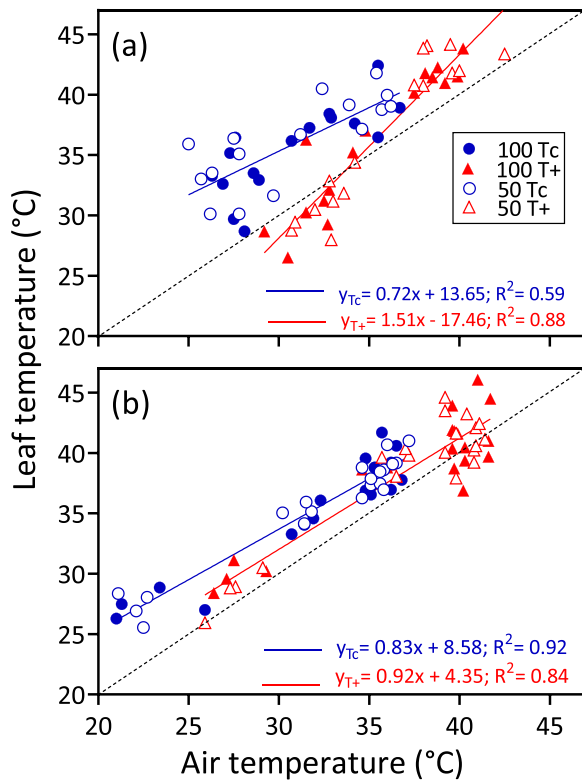


**Fig. 8.** Midday leaf temperature as a function of midday air temperature in the different irrigation (100%, 50%) and temperature (near-ambient control, Tc; warming treatment, T+) combinations in (a) two-year-old, cv. Arbequina trees in 2018 and (b) three-year-old, cv. Coratina trees in 2019. The data points represent individual replicates (n = 4 OTC per treatment combination). Measurements at the beginning of the treatment period and from the recovery period after irrigation was restored are not included. The black dashed line is the 1:1 relationship. Linear equations are given for each of the temperature levels (Tc, T+).

management. In Mediterranean Spain, a significant negative relationship was found between maximum daily air temperature and midday  $\Psi_s$  in two out of three experimental orchards (Corell et al., 2016). A recent study using a survey approach with data from several continents observed a similar negative relationship between midday VPD and  $\Psi_s$  when soil moisture was not limiting (Shackel et al., 2021). Such relationships allow for scheduling irrigation based on atmospheric conditions. In our study, midday  $T_{air}$  and  $\Psi_s$  were also negatively related in both years (Fig. 9). Although different  $\Psi_s$  vs.  $T_{air}$  relationships were not detected between temperature levels in 2018 (Fig. 9a), the T+ treatments had more negative values of  $\Psi_s$  than the well-watered, temperature control (100 Tc) for a given midday  $T_{air}$  in 2019. Furthermore, the  $T_{leaf}$  of the warmed treatments was less than that of Tc for the same  $T_{air}$  in both years (Fig. 8). These results suggest some degree of thermal acclimation to warming during the treatment period. It may be that greater leaf cooling occurred for a given  $T_{air}$  via leaf-level or other adjustments, which led to more negative  $\Psi_s$ . Physiological variables have often been reported to acclimate to a new growth temperature in a number of species (Way et al., 2013; Vico et al., 2019). Whole-tree sap flow previously showed some degree of thermal acclimation in warmed olive trees at our location with greater sap flow occurring in warmed than in control trees at a given  $T_{air}$  after several months of warming in the summer and early fall (Miserere et al., 2019a). However, it is recognized that increases in leaf transpiration were only detected in this study towards the beginning of spring when air temperatures were still fairly low (Fig. 6b, d).

The simultaneous evaluation of multiple factors such as water deficit and warming under experimental conditions can provide insight into

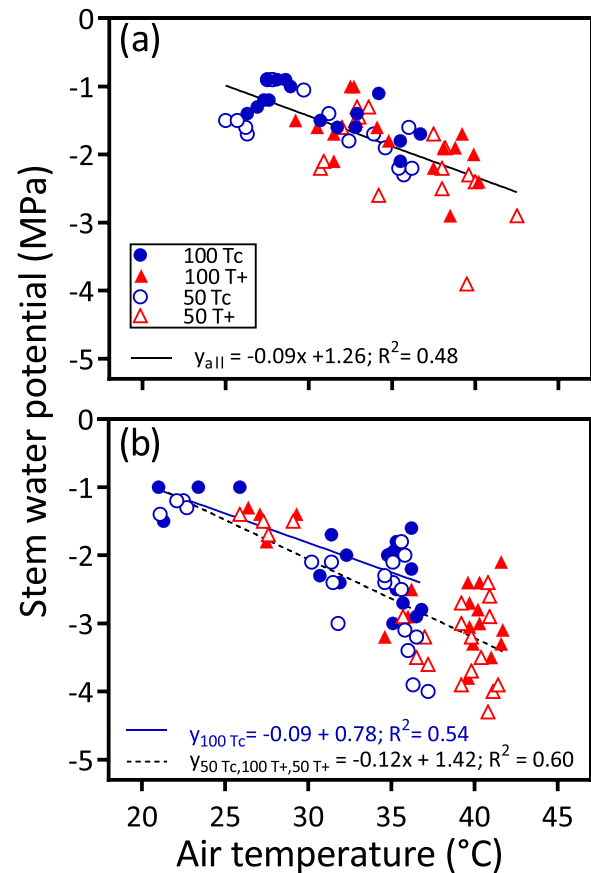


**Fig. 9.** Midday stem water potential as a function of midday air temperature (a, b) in the different irrigation (100%, 50%) and temperature (near-ambient control, Tc; warming treatment, T+) combinations in (a) two-year-old, cv. Arbequina trees in 2018 and (b) three-year-old, cv. Coratina trees in 2019. The data points represent individual replicates (n = 4 OTC per treatment combination). Measurements at the beginning of the treatment period and from the recovery period after irrigation was restored are not included. Linear equations are given for all data combined in 2018 and for specific combinations in 2019.

crop function under climate change (Suzuki et al., 2014; Jagadish et al., 2021). It is important to determine what plant response variables are affected by each factor and what the combined response is. For example; in our study,  $g_s$  was consistently reduced by a moderate water deficit, while warming appeared to have a less pronounced effect on  $g_s$ . In contrast, both water deficit and the + 4 °C warming during the spring combined additively to reduce  $\Psi_s$  even though water deficit reduced transpiring plant leaf area in cv. Arbequina in 2018. In 2019, water deficit did not affect leaf area in cv. Coratina, and warming did not significantly affect leaf area in either year in our study (data not shown). A temperature increase of + 4 °C could occur by 2100 if CO<sub>2</sub> emissions are little controlled (IPCC, 2021). Increased irrigation could be used to mitigate the negative effects of water stress and warming on plant water status (Fraga et al., 2020), but supplemental irrigation is unlikely to be available in all cases. The combined responses to water deficit and warming may be most felt in small, traditional orchards that are rain fed and do not have the possibility of obtaining supplemental irrigation. Increasing atmospheric CO<sub>2</sub> could ameliorate such effects through stomatal closure (Mairech et al., 2021), and experimental studies combining CO<sub>2</sub> with other climate factors are urgently needed for olive trees.

## 5. Conclusions

This is the first experimental study to assess the responses of olive

trees during the spring to the combination of moderate deficit irrigation and warming (4 °C) under natural temperature fluctuations. The results indicate that modifications in water management with global warming will likely be required given the mostly negative individual or additive effects of irrigation deficit and increased air temperature on  $\Psi$ s and other variables. Further studies should focus on plant growth, reproductive development, and oil yield responses to water deficit and warming during the spring.

## Declaration of Competing Interest

The authors declare the following financial interests/personal relationships which may be considered as potential competing interests: Peter S. Searles reports financial support and administrative support were provided by the Argentina Ministry of Science, Technology and Innovation. Maria Cecilia Rousseaux reports financial support and administrative support were provided by the Argentina National Scientific and Technical Research Council.

## Data availability

Data will be made available on request.

## Acknowledgments

Carlos Herrera, Federico Ladux, Hernan Sanmartin and Celeste Gómez provided technical assistance in the field. Fabián Terán of the San Gabriel nursery donated the olive trees. Andrea Miserere provided valuable comments on the experimental set up. This research was supported by grants from the Argentina Ministry of Science, Technology and Innovation (ANPCyT, PICT2015 0195) and the Argentina National Scientific and Technical Research Council (CONICET, PUE 2016 0125). MAI held doctoral fellowships from ANPCyT and CONICET. MCR and PSS are career members of CONICET.

## References

- Agüero Alcaras, L.M., Rousseaux, M.C., Searles, P.S., 2016. Responses of several soil and plant indicators to post-harvest regulated deficit irrigation in olive trees and their potential for irrigation scheduling. *Agric. Water Manag.* 171, 10–20. <https://doi.org/10.1016/j.agwat.2016.03.006>.
- Agüero Alcaras, L.M., Rousseaux, M.C., Searles, P.S., 2021. Yield and water productivity responses of olive trees (cv. Manzanilla) to post-harvest deficit irrigation in a non-Mediterranean climate. *Agric. Water Manag.* 245, 106–162. <https://doi.org/10.1016/j.agwat.2020.106562>.
- Ahumada-Orellana, L., Ortega-Farías, S., Poblete-Echeverría, C., Searles, P.S., 2019. Estimation of stomatal conductance and stem water potential threshold values for water stress in olive trees (cv. Arbequina). *Irrig. Sci.* 37, 461–467. <https://doi.org/10.1007/s00271-019-00623-9>.
- Ahumada-Orellana, L., Ortega-Farías, S., Searles, P.S., Zúñiga, M., 2022. Leaf gas exchange, water status, and oil yield responses to rewetting after irrigation cut-off periods in a superintensive drip-irrigated olive (cv. Arbequina) orchard. *Irrig. Sci.* <https://doi.org/10.1007/s00271-022-00817-8>.
- Ahumada-Orellana, L.E., Ortega-Farías, S., Searles, P.S., Retamales, J.B., 2017. Yield and water productivity responses to irrigation cut-off strategies after fruit set using stem water potential thresholds in a super-high density olive orchard. *Front. Plant Sci.* 8, 1280. <https://doi.org/10.3389/fpls.2017.01280>.
- Araújo, M., Ferreira de Oliveira, J.M.P., Santos, C., Moutinho-Pereira, J., Correia, C., Dias, M.C., 2019. Responses of olive plants exposed to different irrigation treatments in combination with heat shock: physiological and molecular mechanisms during exposure and recovery. *Planta* 249, 1583–1598. <https://doi.org/10.1007/s00425-019-03109-2>.
- Ben-Gal, A., Agam, N., Alchanatis, V., Cohen, Y., Yermiyahu, U., Zipori, I., Presnov, E., Sprintsin, M., Dag, A., 2009. Evaluating water stress in irrigated olives: Correlation of soil water status, tree water status, and thermal imagery. *Irrig. Sci.* 27, 367–376. <https://doi.org/10.1007/s00271-009-0150-7>.
- Benlloch-González, M., Sánchez-Lucas, R., Benlloch, M., Fernández-Escobar, R., 2018. An approach to global warming effects on flowering and fruit set of olive trees growing under field conditions. *Sci. Hortic.* 240, 405–410. <https://doi.org/10.1016/j.scienta.2018.06.054>.
- Benlloch-González, M., Sánchez-Lucas, R., Bejaoui, M.A., Benlloch, M., Fernández-Escobar, R., 2019. Global warming effects on yield and fruit maturation of olive trees growing under field conditions. *Sci. Hortic.* 249, 162–167. <https://doi.org/10.1016/j.scienta.2019.01.046>.
- Berni, J.A.J., Zarco-Tejada, P.J., Sepulcre-Cantó, G., Fereres, E., Villalobos, F., 2009. Mapping canopy conductance and CWSI in olive orchards using high resolution thermal remote sensing imagery. *Remote Sens. Environ.* 113, 2380–2388. <https://doi.org/10.1016/j.rse.2009.06.018>.
- Bongi, G., Mencuccini, M., Fontanazza, G., 1987. Photosynthesis of olive leaves: effect of light flux density, leaf age, temperature, petalates, and H<sub>2</sub>O vapor pressure deficit on gas exchange. *J. Am. Soc. Hortic. Sci.* 112, 143–148. <https://doi.org/10.21273/JASHS.112.1.143>.
- Brito, C., Dinis, L.T., Moutinho-Pereira, J., Correia, C.M., 2019. Drought stress effects and olive tree acclimation under a changing climate. *Plants* 8, 232. <https://doi.org/10.3390/plants8070232>.
- Cabré, F., Nuñez, M., 2020. Impacts of climate change on viticulture in Argentina. *Reg. Environ. Change* 20, 12. <https://doi.org/10.1007/s10113-020-01607-8>.
- Chaves, M.M., Costa, J.M., Zarrouk, O., Pinheiro, C., Lopes, C.M., Pereira, J.S., 2016. Controlling stomatal aperture in semi-arid regions—The dilemma of saving water or being cool? *Plant Sci.* 251, 54–64. <https://doi.org/10.1016/j.plantsci.2016.06.015>.
- Corell, M., Pérez-López, D., Martín-Palomo, M.J., Centeno, A., Girón, I., Galindo, A., 2016. Comparison of the water potential baseline in different locations. Usefulness for irrigation scheduling of olive orchards. *Agric. Water Manag.* 177, 308–316. <https://doi.org/10.1016/j.agwat.2016.08.017>.
- Correa-Tedesco, G., Rousseaux, M.C., Searles, P.S., 2010. Plant growth and yield responses in olive (*Olea europaea*) to different irrigation levels in an arid region of Argentina. *Agric. Water Manag.* 97, 1829–1837. <https://doi.org/10.1016/j.agwat.2010.06.020>.
- Damour, G., Simonneau, T., Cochard, H., Urban, L., 2010. An overview of models of stomatal conductance at the leaf level. *Plant Cell Environ.* 33, 1419–1438. <https://doi.org/10.1111/j.1365-3040.2010.02181.x>.
- Díaz-Espejo, A., Walcroft, A.S., Fernández, J.E., Hafidi, B., Palomo, M.J., Girón, I.F., 2006. Modeling photosynthesis in olive leaves under drought conditions. *Tree Physiol.* 26, 1445–1456. <https://doi.org/10.1093/treephys/26.11.1445>.
- Fereres, E., Orgaz, F., Gonzalez-Dugo, V., 2011. Reflections on food security under water scarcity. *J. Exp. Bot.* 62, 4079–4086. <https://doi.org/10.1093/jxb/err165>.
- Fernández, J.E., 2014. Understanding olive adaptation to abiotic stresses as a tool to increase crop performance. *Environ. Exp. Bot.* 103, 158–179. <https://doi.org/10.1016/j.envexpbot.2013.12.003>.
- Fernández, J.E., Moreno, F., Martín-Palomo, M.J., Cuevas, M.V., Torres-Ruiz, J.M., Moriana, A., 2011. Combining sap flow and trunk diameter measurements to assess water needs in mature olive orchards. *Environ. Exp. Bot.* 72, 330–338. <https://doi.org/10.1016/j.envexpbot.2011.04.004>.
- Fraga, R., Pinto, J.G., Santos, J.A., 2020. Olive tree irrigation as a climate change adaptation measure in Alentejo, Portugal. *Agric. Water Manag.* 237, 106193. <https://doi.org/10.1016/j.agwat.2020.106193>.
- García-Tejera, O., López-Bernal, A., Orgaz, F., Testi, L., Villalobos, F.J., 2021. The pitfalls of water potential for irrigation scheduling. *Agric. Water Manag.* 243, 106522. <https://doi.org/10.1016/j.agwat.2020.106522>.
- García-Tejero, I.F., Hernández, A., Padilla-Díaz, C.M., Díaz-Espejo, A., Fernández, J.E., 2017. Assessing plant water status in a hedgerow olive orchard from thermography at plant level. *Agric. Water Manag.* 188, 50–60. <https://doi.org/10.1016/j.agwat.2017.04.004>.
- Gómez-del-Campo, M., Fernández, J.E., 2007. Manejo del Riego de Olivares en Seto a Partir de Medidas en Suelo y Planta. Editorial Agrícola Española, S.A. Madrid, Spain. <http://hdl.handle.net/10261/176460>.
- Hamze, L.M., Trentacoste, E.R., Searles, P.S., Rousseaux, M.C., 2022. Spring reproductive and vegetative phenology of olive (*Olea europaea* L.) cultivars at different air temperatures along a latitudinal-altitudinal gradient in Argentina. *Sci. Hortic.* 304, 111327. <https://doi.org/10.1016/j.scienta.2022.111327>.
- Haworth, M., Marino, G., Brunetti, C., Killi, D., De Carlo, A., Centritto, M., 2018. The impact of heat stress and water deficit on the photosynthetic and stomatal physiology of olive (*Olea europaea* L.)—a case study of the 2017 heat wave. *Plants* 7, 76. <https://doi.org/10.3390/plants7040076>.
- Hueso, A., Camacho, G., Gómez-del-Campo, M., 2021. Spring deficit irrigation promotes significant reduction on vegetative growth, flowering, fruit growth and production in hedgerow olive orchards (cv. Arbequina). *Agric. Water Manag.* 248, 106695. <https://doi.org/10.1016/j.agwat.2020.106695>.
- Iniesta, F., Testi, L., Orgaz, F., Villalobos, F.J., 2009. The effects of regulated and continuous deficit irrigation on the water use, growth and yield of olive trees. *Eur. J. Agron.* 30, 258–265. <https://doi.org/10.1016/j.eja.2008.12.004>.
- IPCC, 2021. Climate Change 2021: The Physical Science Basis. Contribution of Working Group I to the Sixth Assessment Report of the Intergovernmental Panel on Climate Change. Masson-Delmotte, V., Zhai, P., Pirani, A., Connors, S.L., Péan, C., Berger, S., Caud, N., Chen, Y. (Eds.). IPCC, Switzerland.
- Jagdish, S.V.K., Way, D.A., Sharkey, T.D., 2021. Plant heat stress: Concepts directing future research. *Plant. Cell Environ.* 44, 14050. <https://doi.org/10.1111/pce.14050>.
- Lorite, J.J., Gabaldón-Leal, C., Ruiz-Ramos, M., Belaj, A., de la Rosa, R., León, L., Santos, C., 2018. Evaluation of olive response and adaptation strategies to climate change under semi-arid conditions. *Agric. Water Manag.* 204, 247–261. <https://doi.org/10.1016/j.agwat.2018.04.008>.
- Mairech, H., López-Bernal, A., Moriondo, M., Dibari, C., Regni, L., Proietti, P., Villalobos, F.J., Testi, L., 2021. Sustainability of olive growing in the Mediterranean area under future climate scenarios: Exploring the effects of intensification and deficit irrigation. *Eur. J. Agron.* 129, 126319. <https://doi.org/10.1016/j.eja.2021.126319>.
- Martín-Palomo, M.J., Corell, M., Andreu, L., López-Moreno, E., Galindo, A., Moriana, A., 2021. Identification of water stress conditions in olive trees through frequencies of trunk growth rate. *Agric. Water Manag.* 247, 106735. <https://doi.org/10.1016/j.agwat.2020.106735>.

- Miserere, A., Searles, P.S., Manchó, G., Maseda, P.H., Rousseaux, M.C., 2019a. Sap flow responses to warming and fruit load in young olive trees. *Front. Plant Sci.* 10, 1199. <https://doi.org/10.3389/fpls.2019.01199>.
- Miserere, A., Searles, P.S., Hall, A.J., García-Inza, G.P., Rousseaux, M.C., 2019b. Complementary active heating methods for evaluating the responses of young olive trees to warming. *Sci. Hortic.* 257, 108754. <https://doi.org/10.1016/j.scienta.2019.108754>.
- Miserere, A., Rousseaux, M.C., Ploschuk, E.L., Brizuela, M.M., Curcio, M.H., Zabaleta, R., Searles, P.S., 2021. Effects of prolonged elevated temperature on leaf gas exchange and other leaf traits in young olive trees. *Tree Physiol.* 41, 254–268. <https://doi.org/10.1093/treephys/tpaa118>.
- Miserere, A., Searles, P.S., Rousseaux, M.C., 2022. Oil yield components and biomass production responses to warming during the oil accumulation phase in young olive trees. *Sci. Hortic.* 291, 110618. <https://doi.org/10.1016/j.scienta.2021.110618>.
- Moriana, A., Villalobos, F.J., Fereres, E., 2002. Stomatal and photosynthetic responses of olive (*Olea europaea* L.) leaves to water deficits. *Plant Cell Environ.* 25, 395–405. <https://doi.org/10.1046/j.0016-8025.2001.00822.x>.
- Moriana, A., Pérez-López, D., Prieto, M.H., Ramírez-Santa-Pau, M., Pérez-Rodríguez, J. M., 2012. Midday stem water potential as a useful tool for estimating irrigation requirements in olive trees. *Agric. Water Manag.* 112, 43–54. <https://doi.org/10.1016/j.agwat.2012.06.003>.
- Myers, B.J., 1988. Water stress integral - a link between short-term stress and long-term growth. *Tree Physiol.* 4, 315–323. <https://doi.org/10.1093/treephys/4.4.315>.
- Nissim, Y., Shloberg, M., Biton, I., Many, Y., Doron-Faigenboim, A., Zemach, H., Hovav, R., Kerem, Z., Avidan, B., Ben-Ari, G., 2020. High temperature environment reduces olive oil yield and quality. *One* 15, e02319561–24. <https://doi.org/10.1371/journal.pone.0231956>.
- Pierantozzi, P., Torres, M., Lavee, S., Maestri, D., 2014. Vegetative and reproductive responses, oil yield and composition from olive trees (*Olea europaea*) under contrasting water availability during the dry winter-spring period in central Argentina. *Ann. Appl. Biol.* 164, 116–127. <https://doi.org/10.1111/aab.12086>.
- Pierantozzi, P., Torres, M., Tivani, M., Contreras, C., Gentili, L., Parera, C., Maestri, D., 2020. Spring deficit irrigation in olive (cv. Genovesa) growing under arid continental climate: Effects on vegetative growth and productive parameters. *Agric. Water Manag.* 238, 106212. <https://doi.org/10.1016/j.agwat.2020.106212>.
- Rapoport, H.F., Hammami, S.B.M., Martins, P., Pérez-Priego, O., Orgaz, F., 2012. Influence of water deficits at different times during olive tree inflorescence and flower development. *Environ. Exp. Bot.* 77, 227–233. <https://doi.org/10.1016/j.envexpbot.2011.11.021>.
- Rousseaux, M.C., Benedetti, J.P., Searles, P.S., 2008. Leaf-level responses of olive trees (*Olea europaea*) to the suspension of irrigation during the winter in an arid region of Argentina. *Sci. Hortic.* 115, 135–141. <https://doi.org/10.1016/j.scienta.2007.08.005>.
- Rousseaux, M.C., Figuerola, P.I., Correa-Tedesco, G., Searles, P.S., 2009. Seasonal variations in sap flow and soil evaporation in an olive (*Olea europaea* L.) grove under two irrigation regimes in an arid region of Argentina. *Agric. Water Manag.* 96, 1037–1044. <https://doi.org/10.1016/j.agwat.2009.02.003>.
- Searles, P.S., Alcarás, A., Agüero Alcaras, M., Rousseaux, M.C., 2011. Consumo del agua por el cultivo del olivo (*Olea europaea* L.) en el noroeste de Argentina: una comparación con la Cuenca Mediterránea. *Ecol. Austral* 21, 15–28. (<http://ojs.ecologiaaustral.com.ar/index.php/EcologiaAustral/article/view/1293/663>).
- Sepulcre-Cantó, G., Zarco-Tejada, P., Jiménez-Muñoz, J., Sobrino, J., de Miguel, E., Villalobos, F., 2006. Detection of water stress in an olive orchard with thermal remote sensing imagery. *Agric. Meteorol.* 136, 31–44. <https://doi.org/10.1016/j.agrformet.2006.01.008>.
- Shackel, K., Moriana, A., Marino, G., Corell, M., Pérez-López, D., Martín-Palomo, M.J., Caruso, T., Marra, F.P., Agüero Alcaras, L.M., Milliron, L., Rosecrance, R., Fulton, A., Searles, P., 2021. Establishing a reference baseline for midday stem water potential in olive and its use for plant-based irrigation management. *Front. Plant Sci.* 12, 791711. <https://doi.org/10.3389/fpls.2021.791711>.
- Suzuki, N., Rivero, R.M., Shulaev, V., Blumwald, E., Mittler, R., 2014. Abiotic and biotic stress combinations. *N. Phytol.* 203, 32–43. <https://doi.org/10.1111/nph.12797>.
- Tanasijevic, L., Todorovic, M., Pereira, L.S., Pizzigalli, C., Lionello, P., 2014. Impacts of climate change on olive crop evapotranspiration and irrigation requirements in the Mediterranean region. *Agric. Water Manag.* 144, 54–68. <https://doi.org/10.1016/j.agwat.2014.05.019>.
- Torres, M., Pierantozzi, P., Searles, P., Cecilia Rousseaux, M., García-Inza, G., Miserere, A., Bodoira, R., Contreras, C., Maestri, D., 2017. Olive cultivation in the southern hemisphere: Flowering, water requirements and oil quality responses to new crop environments. *Front. Plant Sci.* 8, 1830. <https://doi.org/10.3389/fpls.2017.01830>.
- Trentacoste, E.R., Calderón, F.J., Contreras-Zanessi, O., Galarza, W., Banco, A.P., Puertas, C.M., 2019. Effect of regulated deficit irrigation during the vegetative growth period on shoot elongation and oil yield components in olive hedgerows (cv. Arbosana) pruned annually on alternate sides in San Juan, Argentina. *Irrig. Sci.* 37, 533–546. <https://doi.org/10.1007/s00271-019-00632-8>.
- Vico, G., Way, D.A., Manzoni, S., 2019. Can leaf net photosynthesis acclimate to rising and more variable temperatures. *Plant Cell Environ.* 42, 1913–1928. <https://doi.org/10.1111/pce.13525>.
- Villalobos, F.J., López-Bernal, A., 2017. Clima. In: Barranco, D., Fernández-Escobar, R., Rallo, L. (Eds.), *El Cultivo del Olivo*, 7th edition., Mundiprensa, Madrid, pp. 213–249.
- Vuletin Selak, G., Perica, S., Goreta Ban, S., Poljak, M., 2013. The effect of temperature and genotype on pollen performance in olive (*Olea europaea* L.). *Sci. Hortic.* 156, 38–46. <https://doi.org/10.1016/j.scienta.2013.03.029>.
- Vuletin Selak, G., Cuevas, J., Goreta Ban, S., Pinillos, V., Domicic, G., Perica, S., 2014. The effect of temperature on the duration of the effective pollination period in 'Oblica' olive (*Olea europaea*) cultivar. *Ann. Appl. Biol.* 164, 85–94. <https://doi.org/10.1111/aab.12082>.
- Way, D.A., Domec, J., Jackson, R.B., 2013. Elevated growth temperatures alter hydraulic characteristics in trembling aspen (*Populus tremuloides*) seedlings: implications for tree drought tolerance. *Plant Cell Environ.* 36, 103–115. <https://doi.org/10.1111/j.1365-3040.2012.02557.x>.
- Zaninelli, P.G., Menéndez, C.G., Falco, M., López-Franca, N., Carril, A.F., 2019. Future hydroclimatic changes in South America based on an ensemble of regional climate models. *Clim. Dyn.* 52, 819–830. <https://doi.org/10.1007/s00382-018-4225-0>.